

## ORIGINAL ARTICLE

# *Pdxdc1* modulates prepulse inhibition of acoustic startle in the mouse

LA Feldcamp<sup>1,2</sup>, PC Boutros<sup>3,4</sup>, R Raymond<sup>5</sup>, PJ Fletcher<sup>2,6,7</sup>, JN Nobrega<sup>5,6,7,8</sup> and AHC Wong<sup>1,2,7,8</sup>

Current antipsychotic medications used to treat schizophrenia all target the dopamine D2 receptor. Although these drugs have serious side effects and limited efficacy, no novel molecular targets for schizophrenia treatment have been successfully translated into new medications. To identify novel potential treatment targets for schizophrenia, we searched for previously unknown molecular modulators of acoustic prepulse inhibition (PPI), a schizophrenia endophenotype, in the mouse. We examined six inbred mouse strains that have a range of PPI, and used microarrays to determine which mRNA levels correlated with PPI across these mouse strains. We examined several brain regions involved in PPI and schizophrenia: hippocampus, striatum, and brainstem, found a number of transcripts that showed good correlation with PPI level, and confirmed this with real-time quantitative PCR. We then selected one candidate gene for further study, *Pdxdc1* (pyridoxal-dependent decarboxylase domain containing 1), because it is a putative enzyme that could metabolize catecholamine neurotransmitters, and thus might be a feasible target for new medications. We determined that *Pdxdc1* mRNA and protein are both strongly expressed in the hippocampus and levels of *Pdxdc1* are inversely correlated with PPI across the six mouse strains. Using shRNA packaged in a lentiviral vector, we suppressed *Pdxdc1* protein levels in the hippocampus and increased PPI by 70%. Our results suggest that *Pdxdc1* may regulate PPI and could be a good target for further investigation as a potential treatment for schizophrenia.

*Translational Psychiatry* (2017) **7**, e1125; doi:10.1038/tp.2017.85; published online 9 May 2017

## INTRODUCTION

Schizophrenia is the ninth leading cause of years lost to disability in established market economies,<sup>1</sup> yet there have been no new pharmacological targets for treating schizophrenia since the discovery of chlorpromazine in 1950.<sup>2</sup> All current antipsychotic medications target the dopamine D2 receptor<sup>3,4</sup> and are effective for reducing hallucinations and delusions,<sup>5</sup> but have little benefit for cognitive impairment or negative symptoms of schizophrenia such as impaired motivation and social withdrawal.<sup>6</sup> This narrow efficacy means that existing medication treatments do not significantly improve overall functioning or outcome in schizophrenia.<sup>7,8</sup> The identification of new molecular pathways for treating schizophrenia is one step towards improving this situation.

We sought to discover novel potential drug targets for antipsychotic drug development by searching for mRNA transcripts that modulate the most commonly studied endophenotype for schizophrenia: prepulse inhibition of the acoustic startle reflex (PPI).<sup>9</sup> Endophenotypes are heritable 'intermediate' phenotypes that constitute a component of a disease, but which may not necessarily be part of the diagnosis.<sup>10</sup> Current psychiatric diagnoses are heterogeneous, have complex genetic origins,<sup>11</sup> and do not correspond to specific neurobiological pathways,<sup>12</sup> which complicates efforts to understand the origins and pathophysiology of mental illnesses. Endophenotypes can help resolve the molecular mechanisms underlying specific elements of

complex psychiatric disorders, through human genetic studies of the endophenotype and animal studies to investigate the molecular and cellular regulation of the endophenotype.<sup>13</sup>

PPI is a measure of sensorimotor gating that is typically measured by exposing an animal to a series of auditory stimuli loud enough to induce a startle response. When lower-intensity 'prepulse' sounds precede a louder 'pulse' sound, PPI reduces the startle response elicited by the second sound.<sup>14</sup> Reduced PPI is manifested as a greater startle response with the same pre-pulse sound. PPI is reduced in a number of neuropsychiatric disorders including schizophrenia, obsessive-compulsive disorder and autism, so is not a diagnosis-specific endophenotype.<sup>15</sup> However, PPI is also reduced in unaffected first-degree relatives of patients with schizophrenia, and in patients with schizophrenia spectrum diagnoses such as schizotypal personality disorder, suggesting that impaired PPI represents a phenotype that is inherited along with schizophrenia.<sup>16</sup> Because PPI can be reliably measured in both the mouse and in humans, and because sensory gating deficits are present in schizophrenia and ameliorated by antipsychotic medication, we reasoned that discovering novel molecular regulators of PPI in the mouse could provide new therapeutic targets to treat symptoms of schizophrenia.<sup>17</sup>

Our strategy was to exploit the variation in PPI levels across different but closely-related mouse strains to identify mRNA transcripts that showed variation in expression level correlated with PPI. A similar approach was used previously to identify

<sup>1</sup>Institute of Medical Science, University of Toronto, Toronto, ON, Canada; <sup>2</sup>Campbell Family Mental Health Research Institute, The Centre for Addiction and Mental Health, Toronto, ON, Canada; <sup>3</sup>Ontario Institute for Cancer Research, Toronto, ON, Canada; <sup>4</sup>Department of Medical Biophysics, University of Toronto, Toronto, ON, Canada; <sup>5</sup>Neuroimaging Section, The Centre for Addiction and Mental Health, Toronto, ON, Canada; <sup>6</sup>Department of Psychology, University of Toronto, Toronto, ON, Canada; <sup>7</sup>Department of Psychiatry, University of Toronto, Toronto, ON, Canada and <sup>8</sup>Department of Pharmacology and Toxicology, University of Toronto, Toronto, ON, Canada. Correspondence: Dr AHC Wong, The Centre for Addiction and Mental Health, Campbell Family Mental Health Research Institute, 250 College Street, Toronto, ON, Canada M5T 1R8. E-mail: albert.wong@utoronto.ca

Received 14 May 2016; revised 11 March 2017; accepted 16 March 2017

*glyoxalase 1* and *glutathione reductase 1* as novel genes regulating anxiety, by examining anxiety behaviors across different mouse strains.<sup>18</sup> We used expression microarrays for this initial screen and real-time quantitative PCR to verify the amount of selected transcripts. Finally, we chose *Pdxdc1*, which encodes a putative decarboxylase, for further study because a soluble enzyme with possible roles in neurotransmitter metabolism is a feasible drug target. *Pdxdc1* mRNA levels were inversely correlated with PPI level, so we used shRNA to knock down *Pdxdc1* levels and saw a corresponding increase in PPI levels in c57BL/6J mice.

## MATERIALS AND METHODS

See Supplementary Material for additional details.

### Mice and PPI testing

Six mouse strains were used: C3H/HeJ, BALB/cJ, C57BLKS/J, C57BL/10J, C57BL/6J and C57L/J (JAX, Bar Harbor, ME, USA) spanning the range of PPI.<sup>19</sup> PND40 mice were housed 6 per cage with a 12 h light/dark cycle (0700–1900 h), at 21 ± 1 °C, 50–60% humidity, food and water *ad libitum*. PPI testing used 120 dB (40 ms) startle (PA), 20 ms prepulses of 75 or 80 dB (PP), 65 dB background, prepulse-startle latency of 100 ms, and inter-trial time of 15–30 s. Scores were averaged across three sessions, PPI calculated as [(PA–PP)/(PA)] × 100, and the mean of 75 and 80 dB trials was used. Six of 12 mice were tested per strain every other day for 5 days at PND50.

### Microarray mRNA transcript analysis

Mice were killed on PND60. Whole striatum, hippocampus, and brainstem were dissected and snap frozen (–80 °C). RNA was prepared as previously described using TRIzol reagent (Invitrogen, Mississauga, ON, Canada).<sup>20</sup> Affymetrix mouse genome MOE 430 2.0 GeneChip arrays were used to measure the mRNA levels of > 34 000 genes using 45 037 probesets. Three arrays were used per strain, per tissue, with pooled RNA samples. Hybridization and imaging was performed by The Centre for Applied Genomics (Toronto, ON, Canada). Transcriptome-wide correlation analysis between PPI and mRNA relied on Spearman's rho and linear modeling analysis, simultaneously fitting 18 arrays per tissue to the model:  $y = b + (m) \times (\text{PPI})$ , where  $y$  is GCRMA pre-processed signal intensity,  $b$  the expression level,  $\text{PPI}$  levels for a given strain, and  $m$  is the slope. Probe sets were annotated using Affymetrix NetAffx (v27)<sup>21</sup> and false discovery rate-adjusted  $P$ -values were calculated. Correlations and  $q$ -values were calculated and candidate genes selected on the combined  $q$ -values from the three brain regions using the formula:  $-\log[q(\text{Hippocampus}) \times q(\text{Striatum}) \times q(\text{Brainstem})]$ . Microarray data were uploaded to the NCBI Gene Expression Omnibus (GEO) under the accession number GSE97198.

### RT-PCR verification of microarray results

mRNA was reverse-transcribed using the Omniscript RT kit with 5 µg RNA. Control genes: GAPDH and  $\beta$ -actin (#4308313 and #4352933E TaqMan Gene Expression Assays, Applied Biosystems, Foster City, CA, USA). Relative mRNA expression was calculated as: [candidate gene]/[geometric mean of GAPDH and  $\beta$ -actin  $C_T$  values].<sup>22</sup> Regression coefficients were calculated using the Standard Curve Method.<sup>23</sup> Array and RT-PCR values were compared by Spearman correlation, then correlated with PPI scores.

### PDXDC1 cloning and Western blots

Human PDXDC1 cDNA (GenBank: BC060871) was cloned into pMCSG53 and expressed in *E.coli* BL21 DE3. Protein growth and purification were as previously described.<sup>24</sup> Protein was quantified before being loaded onto a gel then transferred onto nitrocellulose before staining with Rabbit anti-Pdxdc1 (Abcam, Cambridge, UK, ab83209) or Rabbit anti- $\beta$ -actin (Abcam ab8227) then with Goat anti-rabbit HRP IgG (Abcam, ab6721), detected and quantified.

### *In situ* hybridization and immunohistochemistry to visualize anatomy of Pdxdc1 mRNA and protein expression in brain

For *in situ* hybridization (ISH), PND90 male C57BL/6J mice ( $n = 7$ ) were anesthetized with Avertin (Sigma-Aldrich, Oakville, ON, Canada) then transcardially perfused with saline. Brains were removed and frozen. Twenty micrometer sections were thaw-mounted onto slides.<sup>25</sup>

Densitometry was performed with MCID 7.0 (InterFocus). Raw optical density was converted to  $\mu\text{Ci g}^{-1}$  via calibrated standards. Regions were sampled in 4–5 sections per mouse. For immunohistochemistry (IHC), PND90 male C57BL/6J mice ( $n = 6$ ) were prepared as above, then perfused with 4% PFA. Forty micrometer sections were stained with Rabbit anti-Pdxdc1 (Abcam, ab83209), then biotinylated anti-rabbit IgG conjugated with ABC-HRP, developed with DAB Peroxidase with nickel and float mounted. Raw optical density measures were taken as for ISH. ISH and IHC values were compared in each region to the mean; linear regression and correlational analyses were performed.

### Lentiviral shRNA preparation and brain injection

PND63 male C57BL/6J mice were housed 1 week at The Centre for Phenogenomics (TCP; Toronto, ON, Canada), 5 mice per cage with 12 h light-dark cycle (0700–1900), 50–60% humidity, at 21 ± 1 °C, with *ad libitum* food and water. Mice were pre-tested for PPI, then injected with virus. Experiments were conducted as per Figure 1a. GIPZ constructs for mouse *Pdxdc1* shRNAmir V2LMM\_63165, V3LMM\_453828, non-silencing GIPZ shRNAmir negative control RHS4346 (Thermo Fisher Scientific, Waltham, MA, USA) were prepared as per kit directions and sent to SIDNET (The Hospital for Sick Kids, Toronto, ON, Canada) for packaging with Open Biosystems TransLenti Viral GIPZ Packaging System (Thermo Fisher Scientific). Production, concentration and titering were as per the GIPZ lentiviral product manual. Titters:  $1.64 \times 10^9$  TU ml<sup>-1</sup> (V2LMM\_63165),  $1.02 \times 10^9$  TU ml<sup>-1</sup> (V3LMM\_453828), and  $2.1 \times 10^8$  TU ml<sup>-1</sup> (RHS4346).

**Surgery and infusion.** Mice were anesthetized with isoflurane. A 26 ga non-coring needle delivered 2.5 µl of virus – 2.5 mm from brain surface; sham surgeries were made without injection. Mice were group housed and recovered for 2 weeks before testing.

### Behavior testing after shRNA injection

**Prepulse inhibition.** PPI testing was modified from previous reports.<sup>26</sup> Testing consisted of: pulse alone (PA), pulse+prepulse (PP81dB, PP73dB and PP69dB), prepulse alone or no stimulus (NS) (65 dB) with 90 trials per session. Mice were tested six times, once weekly.

**Locomotor activity.** Mice were tested 1 h in 120 lux Plexiglas locomotor boxes with automated beam break recording.

**Y-maze and spontaneous alternation.** Spontaneous alternation was measured in 5 min periods as previously described.<sup>27</sup>

**Morris water maze.** Morris water maze protocol was modified from previous reports.<sup>28,29</sup> A 1.2 m diameter, 0.5 m deep circular pool filled with water (23–24 °C), clouded with non-toxic paint. A transparent platform 12 cm diameter, 0.35 m high placed in the centre of the southeast quadrant of the tank, peripheral optical markers were used. Mice were pre-tested, then trained for 6 days and probed on day 7.

### Statistical analyses

One or two-way analysis of variance (ANOVA) with Tukey HSD or Bonferroni correction for multiple testing, Student's paired or unpaired two-tailed  $t$ -tests with or without Welch's correction using SPSS 15 or 17. Graphs and some analyses were made using GraphPad Prism 5.0 (La Jolla, CA, USA).

### Tissue analysis after lentiviral shRNA brain injection

IHC was used to determine shRNA localization and protein knockdown. Mice recovered for 24 h after the last behavioral test, and brains were collected, prepared, sectioned and stained as previously described. Tissue from each brain was divided between rabbit anti-tGFP (Pierce Antibodies, Thermo Fisher Scientific, PA5-22688) and rabbit anti-Pdxdc1 (Abcam, ab83209). Sections were observed for tGFP distribution and for *Pdxdc1* staining density in the tissue. Densitometry was conducted as previously described. Western blots and real-time RT-PCR were used to quantify protein and mRNA knockdown.

**Western blot.** Twenty-five micrograms of total protein was loaded per well, and blotting was conducted as above, probing for *Pdxdc1* and  $\beta$ -actin. Protein quantity was analyzed with ImageLab (Bio-Rad Laboratories,

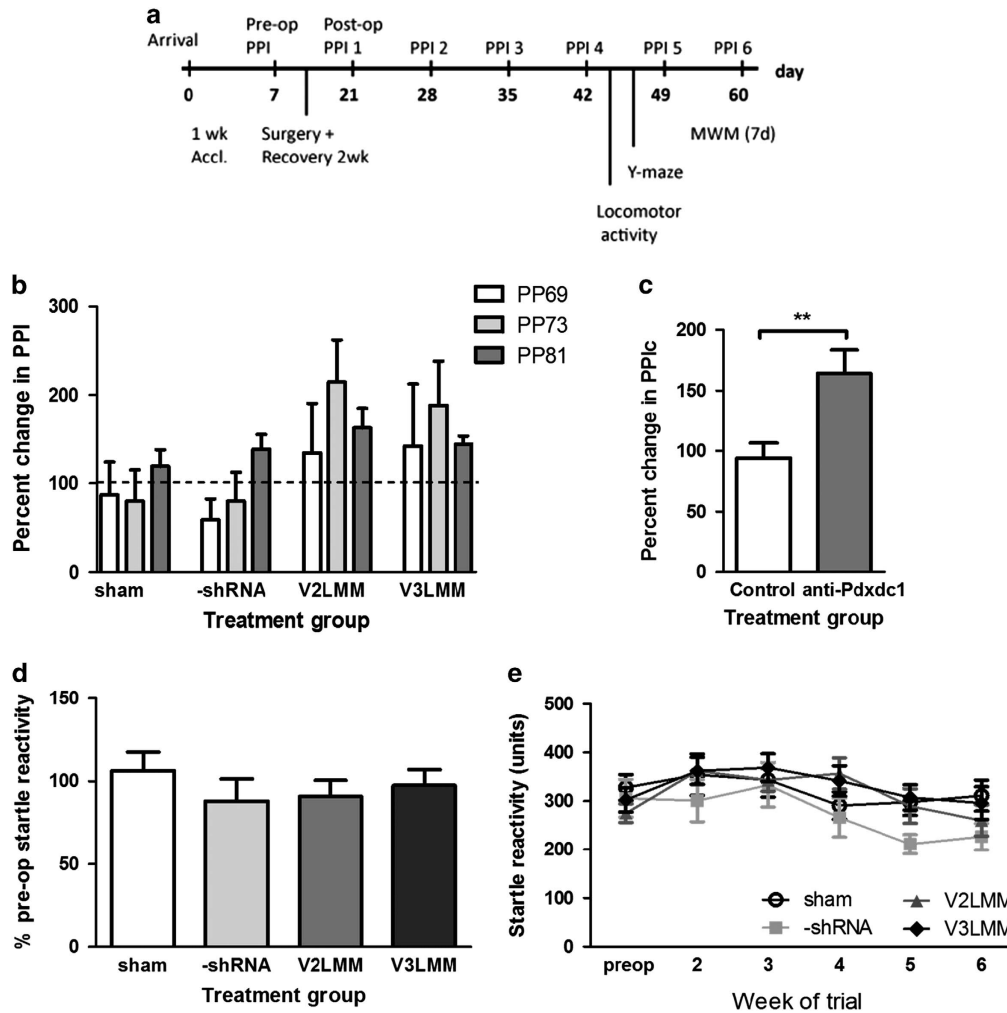


**Figure 1.** *Pdxdc1* knockdown increases PPI but not acoustic startle. All figures show percent change in prepulse inhibition (PPI) from week 2 to 5 after surgery. (a) Surgery and testing timeline from arrival at 9 weeks old until death. (b) Three prepulse intensities (PP69, 73, 81) were tested in every treatment group: one-way ANOVA with each prepulse level showed no significant differences. (c) Combining treatment groups and prepulse intensities showed a significant increase in PPI after *Pdxdc1* knockdown (PPIc refers to combined PPI levels for all prepulse intensities and treatment groups; shown is the percent change in PPIc after surgery:  $**P = 0.0025$ ). (d) There was no statistically significant difference in startle response between groups (shown as percentage of startle before surgery). (e) Longitudinal measurement of startle response from week 1–6. Number of mice per group: sham = 20, -shRNA = 15, V2LMM = 20, V3LMM = 22. ANOVA, analysis of variance.

Mississauga, ON, Canada, v.1.4): absolute protein levels were quantified from digital blot image, and *Pdxdc1* normalized to  $\beta$ -actin in the same lane. Normalized values were averaged and compared between treatment groups. Real-time RT-PCR was conducted as above.

## RESULTS

### Baseline PPI results

A range of PPI levels across strains was seen, with C3H/HeJ mice having the highest, and the three C57BL substrains having the lowest PPI. The overall strain order of PPI is similar to that reported by Willott *et al.*,<sup>19</sup> with the exception that they reported C57L/J to have the highest PPI, and C3H/HeJ was the next highest. The C57BL/10J and C37BLKS/J strains showed very similar and low PPI in both our data and in Willott *et al.*, but in our data the order is reversed. Note that in Willott *et al.*, the strain order differed slightly when different frequencies (pitch) of startle stimuli were used, although the broad patterns were conserved. One-way ANOVA showed significant differences in the combined PPI values across all six strains (Figure 2a;  $F_{5,28} = 10.78$ ,  $P < 0.0001$ , post hoc Tukey's HSD), with differences specifically between C3H/HeJ vs Balb/cJ

( $*P < 0.01$ ), vs C57BL/6J ( $**P < 0.001$ ), vs C57BL/10J ( $**P < 0.001$ ) and vs C57BLKS/J ( $**P < 0.001$ ). The ASR was lower in C57L/J and C3H/HeJ compared to the other four strains ( $F_{5,30} = 29.73$ ,  $P < 0.0001$ , post hoc Tukey's HSD showing  $P < 0.0001$ ) however, PPI had no correlation with startle (data not shown).

### Microarray results

Linear-modeling analysis of mRNA expression with PPI generated 535 differentially expressed ( $q > 0.01$ ) annotated probe sets in hippocampus, 528 in brainstem and 1149 in striatum. There were 314 probe sets in common between the three tissues (Figure 2b). Probe sets were chosen for RT-PCR validation based on several criteria: (1) the  $q$ -value; (2) relatively high expression levels; and (3) the correlation between PPI and transcript level. Transcripts with multiple probe sets meeting these criteria were given priority as well as transcripts encoding soluble cytosolic proteins since these are more feasible drug targets than structural proteins for example. A selection of high-priority transcripts are shown in Supplementary Figure S1A. The genes chosen for PCR verification of RNA levels were *Rgs5*, *Dbdd2*, *Hist1h2bc*, *Pdxdc1*, and *Dnm3*. No

significant differences were seen in overall expression levels across arrays and between groups exposed to PPI testing and control animals left in their home cages (Supplementary Figure S2).

Real-time RT-PCR verification of mRNA levels

The strongest correlation between mRNA levels measured by PCR and PPI was for *Pdxd1* in hippocampus ( $P=0.03$ , Figure 2c). There

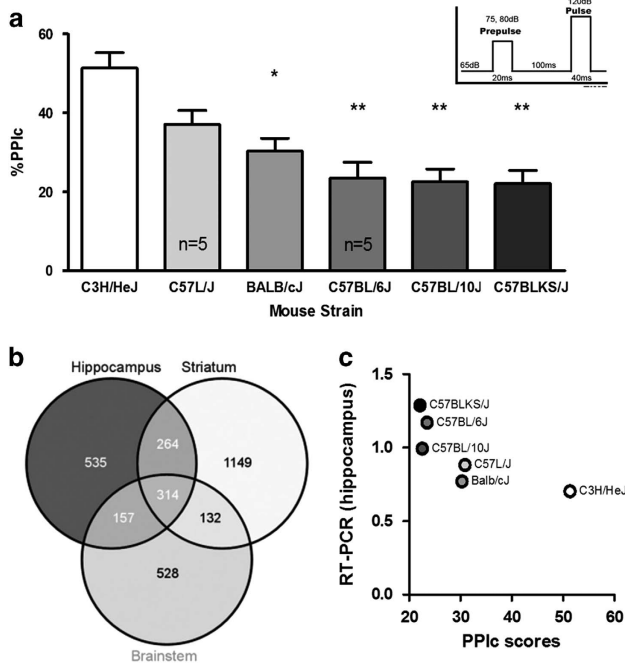


**Figure 2.** Selection of *Pdxd1* as a candidate transcript for regulating PPI. (a) PPI in six different mouse strains ( $n = 34$  mice total). One-way ANOVA for PPIc between all groups showed significant differences ( $F_{5,28} = 10.78$ ,  $P < 0.0001$ , *post hoc* with Tukey's HSD) between C3H/HeJ vs Balb/cJ ( $*P < 0.01$ ), vs C57BL/6J ( $**P < 0.001$ ), vs C57BL/10J ( $**P < 0.001$ ), and vs C57BLKS/J ( $**P < 0.001$ ). PPIc represents the mean PPI for 75 and 80 dB startle intensities. (b) Venn diagram showing overlap between brain regions in transcripts that have levels correlated with PPI. The number of microarray probesets associated with PPI in each region and in common between regions are listed. (c) PPI and *Pdxd1* mRNA levels in the hippocampus are inversely correlated ( $n = 3$  mice per strain per tissue; Spearman's  $\rho = -0.8557$ ,  $P = 0.03$ ). Data shown are from real-time RT-PCR for *Pdxd1* mRNA quantification. The strain order for *Pdxd1* mRNA levels mirrors the strain order for PPIs in a. ANOVA, analysis of variance; PPI, prepulse inhibition.

was also good correlation for *Hist1h2bc* in brainstem and hippocampus ( $P=0.03$ , both tissues), and *Dbndd2* in brainstem ( $P=0.06$ ) but these data were not corrected for multiple testing (Supplementary Figure 1b). *Pdxd1* mRNA levels in each strain also matched their ordering by PPI. These results confirmed that the microarray analysis was able to identify a gene that was expressed at high levels in strains of mice with low PPI and vice versa.

Anatomy of *Pdxd1* expression in the brain

DAB IHC was used to visualize *Pdxd1* protein expression and ISH was used to observe mRNA expression in adult mouse brain slices. Considerable regional variation was seen in *Pdxd1* expression (Figure 3a). Thirty-one regions known to have some role in PPI were sampled in both IHC (Figure 3b,  $n=6$ ) and ISH (Figure 3c,  $n=7$ ) stained tissue. Hippocampus (CA1, CA2, CA3, and DG) showed the highest levels of both *Pdxd1* protein and mRNA. mRNA and protein levels were consistent for hippocampus, cingulate, pontine nucleus and dorsal raphe nucleus ( $< 2$  s.e.m. difference between protein and mRNA relative to each respective mean), while others were quite divergent ( $> 2$  s.e.m. difference): frontal associative and orbital cortex, striatum (excluding globus pallidus), medial septal nucleus, substantia nigra, central nucleus of inferior colliculus and central cochlear nucleus, anterior part.

For comparison, this analysis was conducted for 73 additional tissue regions not associated with PPI (not shown). As a group, brain areas not directly implicated in regulating PPI actually had slightly higher *Pdxd1* protein levels than those areas implicated in PPI: PPI area mean =  $0.151 \pm 0.003$  (s.e.m.) vs non-PPI mean =  $0.165 \pm 0.005$  (s.e.m.). This was driven by several regions within the prefrontal cortex, mesencephalon, hypothalamus and rhombencephalon. However, the overall expression level in non-PPI areas was more uniform, with few regions deviating more than 2 s.e.m. from the mean of all regions. For mRNA expression, areas implicated in PPI did not differ substantially from the non-PPI regions: PPI mean =  $53.5 \pm 1.37$  (s.e.m.) vs non-PPI mean =  $53.15 \pm 1.97$  (s.e.m.).

Overall there was good correlation between mRNA and protein levels, in both PPI-related and non-PPI regions. PPI-only regions had Spearman  $\rho = 0.7803$  ( $P < 0.0001$ ),  $r^2 = 0.609$  (Figure 3d). The correlation across all regions (Figure 3e) showed Spearman's  $\rho = 0.700$  ( $P < 0.0001$ ),  $r^2 = 0.576$  (not shown). Non-PPI regions showed Spearman's  $\rho = 0.701$  ( $P < 0.0001$ ),  $r^2 = 0.601$  (not shown). Residuals analysis for all combinations were analyzed, showing  $r^2 = 0.000$  for each.

*Pdxd1* protein is knocked down by shRNA *in vivo*

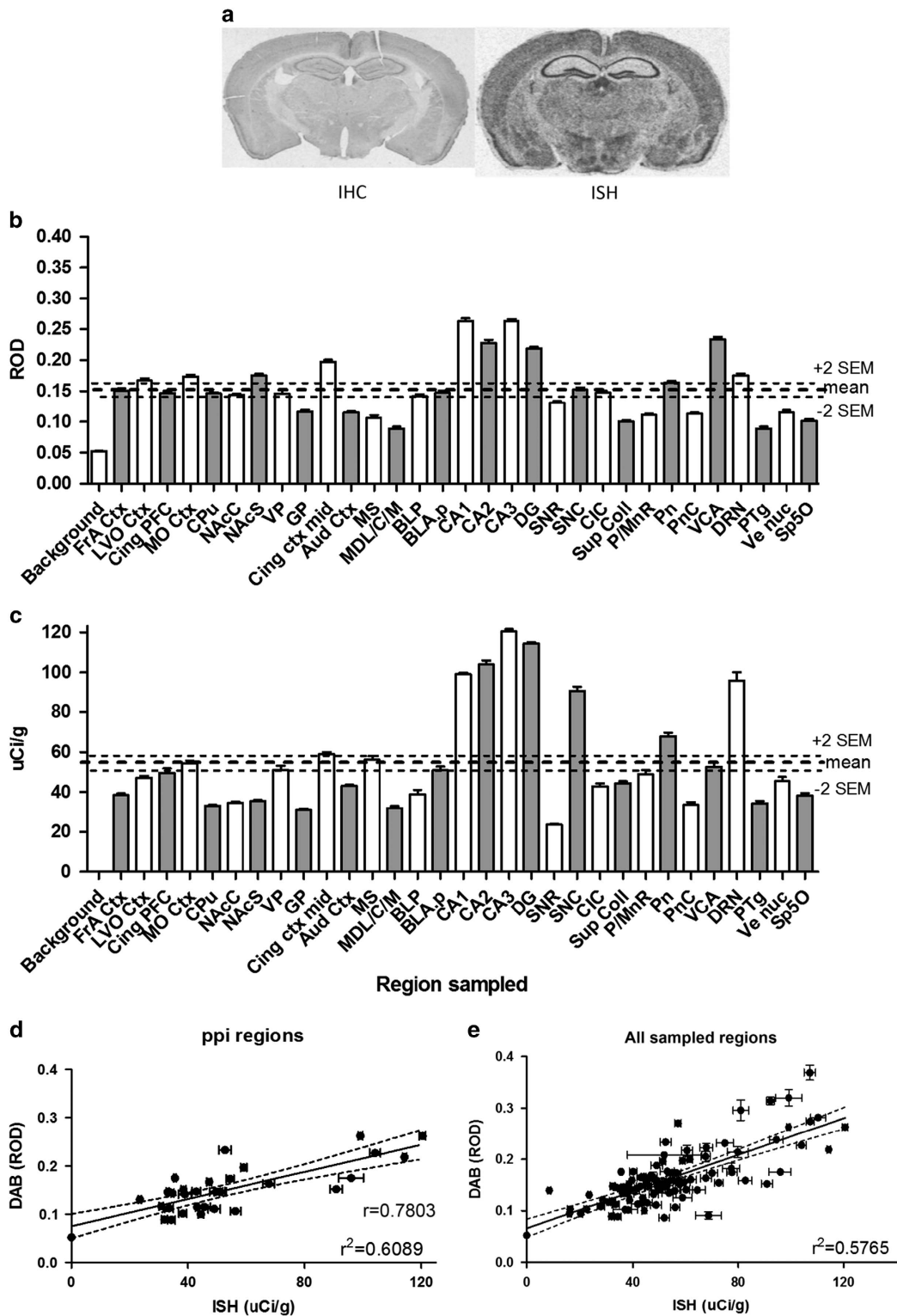
The two anti-*Pdxd1* shRNAs (V2 and V3) were effective in knocking down *Pdxd1*. Infusion of V2, V3 or control shRNA into

**Figure 3.** *Pdxd1* mRNA and protein expression in mouse brain. (a) Sample immunohistochemical (IHC) and *in situ* hybridization (ISH) images for *Pdxd1* protein and mRNA, respectively, from adult male mice using a visible light microscope. (b) *Pdxd1* mRNA expression in PPI-associated brain regions measured with ISH ( $n = 7$  mice) and (c) *Pdxd1* protein expression measured with IHC, in naïve male C57BL/6J mice ( $n = 6$ ) at 12 weeks of age. DAB (IHC): mean =  $0.151 \pm 0.003$  (s.e.m.), 2x.s.e.m. (+) = 0.157 (-) = 0.144. ISH: mean =  $53.5 \pm 1.37$  (s.e.m.), 2x.s.e.m. (+) = 56.2 (-) = 50.7. Thick dotted lines indicate whole brain averages. Thin dotted lines (+2s.e.m., -2s.e.m.) represent the whole brain confidence interval (at 2x.s.e.m.) for the mean. (d) PPI regions linear regression for DAB and ISH:  $r^2 = 0.609$ , SE of the estimate of residuals = 0.032. 95% confidence interval (CI): Slope 0.00099 to 0.00183. Correlation analysis Spearman's  $\rho = 0.706$ , 95% CI: 0.465 to 0.849, two-tailed  $P < 0.0001$  (32 x,y pairs). (e) Linear regression for all sampled regions.  $r^2 = 0.5765$ , 95% CI: 0.0486 to 0.0836 (105 x,y pairs). Correlation analysis: Spearman's  $\rho = 0.7003$ , 95% CI: 0.584 to 0.789, two-tailed  $P < 0.0001$ . Aud Ctx, 1° & 2° auditory ctx; BLP, basolateral amygdala; posterior; BLA.p, basolateral amygdale; anterior; CA1, field CA1 of hippocampus; CA2, field CA2 of hippocampus; CA3, field CA3 of hippocampus; CIC, central nucleus; inferior colliculus; Cing ctx mid, 1° & 2° cingulate ctx areas; Cing PFC, cingulate ctx area1; CPu, caudate putamen; DG, dentate gyrus; DRN, dorsal raphe nucleus; FrA Ctx, frontal association ctx; GP, globus pallidus; LVO ctx, lateral/ventral orbital ctx; MO Ctx, medial orbital ctx; MS, medial septal nucleus; MDL/C/M, mediodorsal thalamic nuclei; NAcC, nucleus accumbens core; NAcS, nucleus accumbens shell; P/MnR, paramedian and medial raphe nuclei; Pn, pontine nucleus; PnC, caudal pontine reticular nucleus; PPI, prepulse inhibition; PTg, pedunculotegmental nucleus; SNC, substantia nigra pars compacta; SNR, substantia nigra pars reticulata; Sp50, spinal trigeminal tract; Sup Coll, superior colliculus; VCA, anterior ventral cochlear nucleus; Ve muc, vestibular nucleus; VP, ventral pallidum.



the DG showed tGFP expression ranging from -1.06 to -3.80 mm bregma in both dorsal and ventral DG in all injected mice (Figure 4a). *Pdxdc1* protein was significantly knocked down in all hippocampal regions by both *Pdxdc1* shRNAs (one-way ANOVA  $F_{3,615} = 34.5$ ,  $P < 0.0001$ ). Tukey's HSD for V2 or V3 vs sham or control shRNA was significant ( $P < 0.0001$ ) for each comparison

across all regions (Figure 4b). V2 shRNA reduced *Pdxdc1* protein in the DG by 40%, while V3 reduced it by 26%. *Pdxdc1* levels were reduced in other hippocampal areas: CA1 - 16%, CA2 - 30.6%, and CA3 - 30%.  $N = 5$  brains per region, 6 sections per brain. Significant differences in expression of *Pdxdc1* existed between groups in CA3 ( $F_{3,352} = 109.1$ ,  $P < 0.0001$ ) with post hoc analysis indicating



differences between V2 and V3 ( $P < 0.001$ ), and sham vs -shRNA ( $P < 0.05$ ). For DG, significant differences were seen ( $F_{552,3} = 192.8$ ,  $P < 0.001$ ) with post hoc analysis showing differences between V2 and V3, and between control and treated groups ( $P < 0.0001$ , each combination).

Western blot confirmed the IHC data, showing a 35.9% reduction of *Pdxd1* by V3 shRNA ( $F_{3,8} = 5.310$ ,  $P = 0.0263$ , one-way ANOVA, Tukey's HSD,  $P < 0.05$ ), and 31.7% by V2 shRNA (Figure 4c). Relative protein expression was calculated comparing *Pdxd1* to  $\beta$ -actin (Figure 4d). *Pdxd1* RNA levels were not reduced by shRNA, measured by real-time RT-PCR, relative to the geometric mean of controls GAPDH and  $\beta$ -actin (Figure 4e).

PPI is increased by *Pdxd1* knockdown

PPI was tested 2 weeks after shRNA injection, and testing continued over 40 days (Figure 1a). The analysis was conducted on the combined anti-*Pdxd1* shRNA groups in comparison to a combined control group of both sham and -shRNA groups (from Figure 1b). PPI levels across all three pre-pulse intensities were combined into a single measure, PPIc. *Pdxd1* knockdown produced a significant increase in PPI compared to the control groups ( $t = 3.064$  df = 205  $P = 0.0025$ , unpaired two-tailed Student's *t*-test, Welch's correction) (Figure 1c). Conversely, there was no significant difference in startle reactivity between treatment groups ( $F_{3,76} = 0.547$ ,  $P = 0.652$ , one-way ANOVA, Tukey's HSD; Figure 1d and e). However, when raw PPI scores are analyzed as a mean of each treatment group as opposed to percentage change in each animal from before and after surgery, there are no significant differences in PPI associated with *Pdxd1* knockdown (Supplementary Figure S4).

Spontaneous locomotor activity was increased by *Pdxd1* knockdown. The anti-*Pdxd1* shRNA mice had greater horizontal activity compared to controls during the first 5 min of testing ( $P < 0.0076$ , Student's unpaired two-tailed *t*-test  $t = 2.743$  df = 78; Figure 5a and b). The same was true for vertical activity over the hour of activity observation (Figure 5c): Student's two-sided *t*-test ( $t = 2.176$  d.f. = 76  $P = 0.0327$ ). There were no significant behavioral differences seen in Y-maze or Morris water maze results (Supplementary Figure S3).

## DISCUSSION

To our knowledge, the experiments described above provide the first evidence that *Pdxd1* may modulate PPI of the acoustic startle response, a measure of sensorimotor gating in the mouse. We first identified a number of gene transcripts that could modulate PPI by measuring brain mRNA levels in six different mouse strains with a range of PPI. We found ~2000 genes with strong correlation between the amount of mRNA and PPI. Five of the transcripts with the strongest correlations were quantified with real-time RT-PCR, and these results were in good agreement with the microarray data. We focused on *Pdxd1* and knocked down the transcript in hippocampus with shRNA. Mice with reduced *Pdxd1* protein after shRNA injection showed increased PPI, consistent with the inverse correlation between PPI and *Pdxd1* mRNA levels seen on the microarrays.

We focused on *Pdxd1* in particular because the mRNA and PPI levels across mouse strains were strongly (inversely) correlated and because this correlation was consistent across hippocampus, striatum and brainstem. The function of *Pdxd1* is unknown but we speculate that it may encode a decarboxylase that is involved in monoamine neurotransmitter synthesis. This makes *Pdxd1* attractive as a potential drug target because a cytosolic enzyme could control neurotransmitter levels, and could be accessible to a small molecule compound. In contrast, genes active during development, or that encode structural proteins, might be less effective as a drug target.

One limitation of our experimental design is that we could have missed other transcripts that modulate PPI because the microarray we used was based on the genome of B6 mouse strains, and could thus potentially miss transcripts that are more strongly expressed in other mouse strains.<sup>30</sup> In cases where there is considerable SNP variability between strains, hybridization artefacts can potentially skew the data.<sup>31</sup> RNA-Seq could be used instead to address this strain bias. However, we used microarrays only as a starting point to identify candidate transcripts, and performed a number of other experiments to verify that *Pdxd1* has an effect on PPI levels.

To investigate the potential role of *Pdxd1* in PPI, we measured *Pdxd1* expression in brain regions involved in regulating PPI. The highest levels of *Pdxd1* protein and mRNA were found in the hippocampus. Lesion and genetic experiments demonstrate that alterations in the hippocampus can affect PPI.<sup>32,33</sup> Furthermore, there was good correlation between protein and mRNA levels in the hippocampus, which was not true in some other brain areas.<sup>34</sup> The observed differences between *Pdxd1* mRNA and protein amount in some brain regions is consistent with a dynamic system modulation function for *Pdxd1* rather than a structural or basic metabolic function.<sup>35,36</sup>

To confirm that *Pdxd1* levels can regulate PPI, we used an engineered lentivirus carrying an shRNA-containing plasmid to knock down *Pdxd1*. PPI increased in mice after *Pdxd1* knockdown, providing experimental evidence that this protein affects PPI and could therefore be a potential target for new antipsychotic medications. The apparent increase in PPI after *Pdxd1* knockdown was only statistically significant when treatment groups were combined into knockdown vs control and when the percent change in PPI in each animal was used as the variable. When raw PPI scores were analyzed, no significant changes with *Pdxd1* knockdown were seen. This likely is due to the high variability in PPI scores between animals.

*Pdxd1* protein levels were significantly reduced after shRNA injection, but mRNA levels were not. It is possible that the shRNA used may have blocked protein production as an miRNA instead of an siRNA, or inhibited protein translation instead of promoting mRNA digestion.<sup>37,38</sup> Expression of the tGFP marker was restricted to the dentate, but *Pdxd1* protein reduction extended more widely throughout the hippocampus. This discrepancy could be related to overall hippocampal function and homeostatic shifts in protein production or inter-individual variability within the tissues sampled. Further experiments would be required to investigate these potential explanations.

*Pdxd1* knockdown did not have strong effects on other behaviors dependent on the hippocampus such as learning and memory, but did increase locomotor activity. Because locomotion is often considered a measure of dopamine system output, *Pdxd1* could be directly or indirectly affecting dopamine signaling.<sup>39</sup> However, decreasing *Pdxd1* levels improved PPI and increased locomotion, while existing antipsychotic medications reduce locomotion.<sup>3</sup> This suggests that *Pdxd1* is not modulating PPI through the same mechanism as current treatments for schizophrenia, but could also be a potential disadvantage if other rodent behaviors linked to schizophrenia are similarly affected.

Our interpretation of the behavioral effects of *Pdxd1* knockdown is hampered by the lack of knowledge about the function of *Pdxd1*. The amino acid homology to existing decarboxylases suggests that *Pdxd1* may be involved in neurotransmitter synthesis. Thus, an important next step is to investigate whether this protein is indeed an enzyme that catalyzes synthesis of neurotransmitters. Subsequent efforts could be directed at resolving the structure of this protein with the aim of developing small molecule inhibitors.

Another obstacle in the quest for better psychiatric drug treatments is the difficulty in translating disease phenotypes into animal model assays.<sup>40</sup> Decreased PPI is often considered a stable

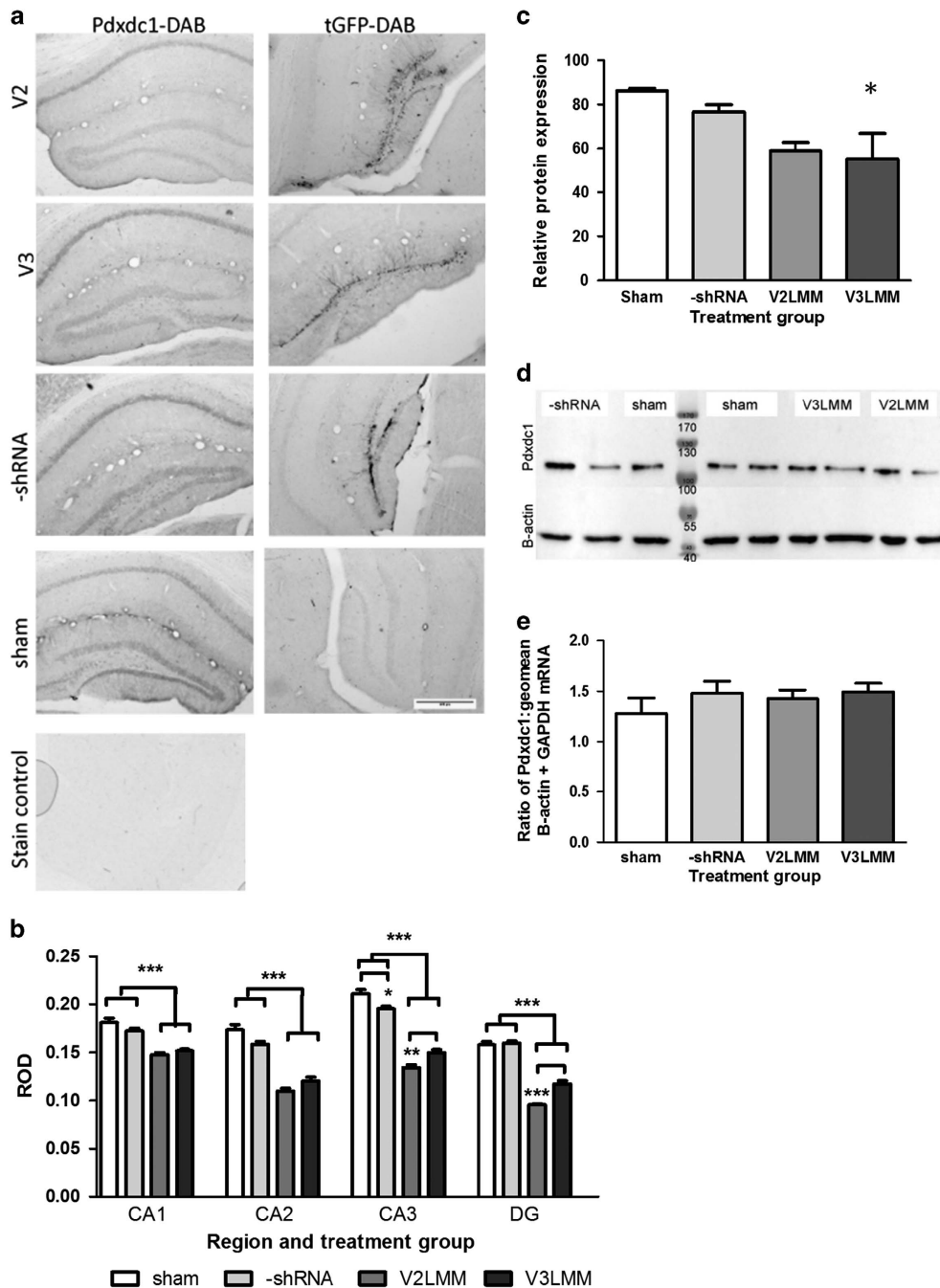


**Figure 4.** Knockdown of *Pdxdc1* *in vivo* with lentiviral shRNA. **(a)** *Pdxdc1*-DAB (left column): Two viral shRNAs, V2LMM (V2) and V3LMM (V3), were used to knock down *Pdxdc1* protein in the dentate gyrus of the hippocampus. *tGFP*-DAB (right column): the DAB stain for *tGFP* showing infected areas using V2LMM, V3LMM, or -shRNA viral vectors. Cell bodies and mossy fibers are prominently stained at 4x optical magnification. The scale bar is 400  $\mu$ m;  $n = 5$  mice per shRNA. **(b)** Significant differences in *Pdxdc1* expression as measured by relative optical density (ROD) were seen between anti-*Pdxdc1* treated groups and controls ( $n = 5$  mice per group). One-way ANOVA for *Pdxdc1* quantity was performed within each tissue region for each treatment group with the Tukey HSD *post hoc* test. CA1 showed a significant difference (ANOVA  $F_{3,615} = 34.50$ ,  $P < 0.0001$ ) with *post hoc* analysis differences between V2 vs sham, V2 vs -shRNA, V3 vs sham, and V3 vs -shRNA groups ( $***P < 0.0001$  each comparison). CA2 had significant differences between groups (ANOVA  $F_{3,215} = 61.75$ ,  $P < 0.0001$ ), and *post hoc* analysis showed highly significant differences ( $***P < 0.0001$ , all comparisons listed: V2 vs sham, V2 vs -shRNA, V3 vs sham, and V3 vs -shRNA groups). CA3 groups were significantly different (ANOVA  $F_{3,352} = 109.1$ ,  $P < 0.0001$ ) with *post hoc* analysis showing differences between V2 vs V3 ( $**P < 0.001$ ), V2 vs sham ( $***P < 0.0001$ ), V2 vs -shRNA ( $P < 0.0001$ ), V3 vs sham ( $P < 0.0001$ ), V3 vs -shRNA ( $P < 0.0001$ ) and between sham vs -shRNA ( $P < 0.05$ ). **(c)** *Pdxdc1* protein levels in dorsal hippocampus normalized to  $\beta$ -actin, showing a significant decrease with the V3LMM shRNA; mean  $\pm$  s.e.m., \* $P < 0.05$ . **(d)** *Pdxdc1* protein from dorsal hippocampus shown on representative Western blot; *Pdxdc1* (top) and  $\beta$ -actin (bottom) for all treatment groups, 2 lanes for each treatment and 3 lanes sham ( $n = 4-5$  mice per treatment group). **(e)** *Pdxdc1* mRNA expression between the four treatment groups, normalized to housekeeping genes. No significant differences were seen between the groups. Data are shown as mean  $\pm$  s.e.m.

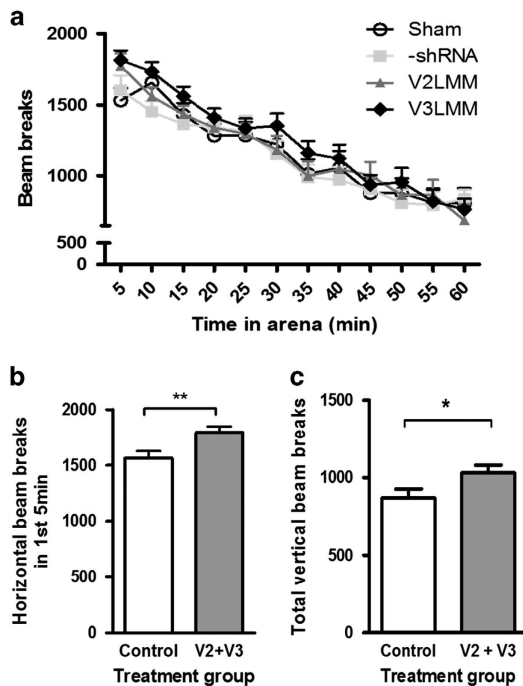


**Figure 5.** *Pdxc1* knockdown increases locomotor activity. (a) Differences in horizontal locomotor activity were seen between sham and V2 groups at 5 min ( $P < 0.05$ ). At 10 min, differences between -shRNA and V3LMM groups ( $P < 0.05$ ) were seen with one-way analysis of variance (ANOVA;  $F_{3,113} = 2.785$ ,  $P = 0.0441$ ) with Tukey's HSD. No other significant differences were seen. (b) Horizontal distance moved in the first 5 min was greater in the *Pdxc1* knockdown group. Combined groups: controls vs anti-*Pdxc1*:  $**P = 0.0076$ , unpaired two-tailed Student's *t*-test. (c) Total vertical activity was greater in the *Pdxc1* knockdown group. Combined group of controls vs anti-*Pdxc1*:  $*P = 0.03$ , unpaired two-tailed Student's *t*-test (sham  $n = 20$ , -shRNA  $n = 10$ , V2LMM  $n = 18$ , V3LMM  $n = 1$ ).

trait endophenotype in schizophrenia spectrum disorders and in unaffected relatives.<sup>10</sup> PPI is also interpreted as a state marker for psychosis—its restoration in animal models by antipsychotic medications<sup>41</sup> is considered a proxy for the acute reduction of psychotic symptoms in patients.<sup>42</sup> In the work described here, we have intentionally applied both of these conceptualizations of PPI. By using differences in PPI across genetically different mouse strains to identify mRNA transcripts regulating PPI, we are explicitly treating PPI as a stable genetically-influenced trait. In contrast, by knocking down *Pdxc1* mRNA with shRNA, and hypothesizing that this should increase PPI, we are making the assumption that PPI can be dynamically regulated and that this could point to antipsychotic-like effects. It would be helpful to have additional animal behavior or biochemical assays with which to predict antipsychotic effects in human patients.<sup>40</sup>

Nevertheless, the results presented here suggest that *Pdxc1* may be a novel modulator of PPI, the most well-known behavioral endophenotype for schizophrenia. Further investigations into the function of *Pdxc1* and the effects of inhibiting *Pdxc1* would be helpful. Because *Pdxc1* is a cytosolic protein with putative catalytic functions that could dynamically modulate neurotransmitter levels, it is an attractive potential target for new antipsychotic medications for treating schizophrenia.

#### CONFLICT OF INTEREST

The authors declare no conflict of interest.

#### ACKNOWLEDGMENTS

We thank Dr Alexander Iakounine and Greg Brown for help in producing human *Pdxc1* protein.

#### REFERENCES

- Vos T, Flaxman AD, Naghavi M, Lozano R, Michaud C, Ezzati M et al. Years lived with disability (YLDs) for 1160 sequelae of 289 diseases and injuries 1990-2010: a systematic analysis for the Global Burden of Disease Study 2010. *Lancet* 2012; **380**: 2163-2196.
- Insel TR, Scolnick EM. Cure therapeutics and strategic prevention: raising the bar for mental health research. *Mol Psychiatry* 2006; **11**: 11-17.
- Seeman P, Lee T. Antipsychotic drugs: direct correlation between clinical potency and presynaptic action on dopamine neurons. *Science* 1975; **188**: 1217-1219.
- Seeman P, Lee T, Chau-Wong M, Wong K. Antipsychotic drug doses and neuroleptic/dopamine receptors. *Nature* 1976; **261**: 717-719.
- Lieberman JA, Stroup TS, McEvoy JP, Swartz MS, Rosenheck RA, Perkins DO et al. Effectiveness of antipsychotic drugs in patients with chronic schizophrenia. *N Engl J Med* 2005; **353**: 1209-1223.
- Wong AH, Van Tol HH. Schizophrenia: from phenomenology to neurobiology. *Neurosci Biobehav Rev* 2003; **27**: 269-306.
- Lang FU, Kosters M, Lang S, Becker T, Jager M. Psychopathological long-term outcome of schizophrenia—a review. *Acta Psychiatr Scand* 2013; **127**: 173-182.
- Jobe TH, Harrow M. Long-term outcome of patients with schizophrenia: a review. *Can J Psychiatry* 2005; **50**: 892-900.
- Braff DL, Grillon C, Geyer MA. Gating and habituation of the startle reflex in schizophrenic patients. *Arch Gen Psychiatry* 1992; **49**: 206-215.
- Gottesman II, Gould TD. The endophenotype concept in psychiatry: etymology and strategic intentions. *Am J Psychiatry* 2003; **160**: 636-645.
- Sullivan PF, Daly MJ, O'Donovan M. Genetic architectures of psychiatric disorders: the emerging picture and its implications. *Nat Rev Genet* 2012; **13**: 537-551.
- Insel T, Cuthbert B, Garvey M, Heinssen R, Pine DS, Quinn K et al. Research domain criteria (RDoC): toward a new classification framework for research on mental disorders. *Am J Psychiatry* 2010; **167**: 748-751.
- Nestler EJ, Hyman SE. Animal models of neuropsychiatric disorders. *Nat Neurosci* 2010; **13**: 1161-1169.
- Geyer MA, Dulawa SC. Assessment of murine startle reactivity, prepulse inhibition, and habituation. *Curr Protoc Neurosci* 2003; **Chapter 8**: Unit 8.17.
- Kohl S, Heekeren K, Klosterkotter J, Kuhn J. Prepulse inhibition in psychiatric disorders—apart from schizophrenia. *J Psychiatr Res* 2013; **47**: 445-452.
- Braff DL, Light GA. The use of neurophysiological endophenotypes to understand the genetic basis of schizophrenia. *Dialogues Clin Neurosci* 2005; **7**: 125-135.
- Swerdlow NR, Weber M, Qu Y, Light GA, Braff DL. Realistic expectations of prepulse inhibition in translational models for schizophrenia research. *Psychopharmacology (Berl)* 2008; **199**: 331-388.
- Hovatta I, Tennant RS, Helton R, Marr RA, Singer O, Redwine JM et al. Glyoxalase 1 and glutathione reductase 1 regulate anxiety in mice. *Nature* 2005; **438**: 662-666.
- Willott JF, Tanner L, O'Steen J, Johnson KR, Bogue MA, Gagnon L. Acoustic startle and prepulse inhibition in 40 inbred strains of mice. *Behav Neurosci* 2003; **117**: 716-727.
- Semerlul MO, Boutros PC, Likhodi O, Okey AB, Van Tol HH, Wong AH. Microarray analysis of the developing cortex. *J Neurobiol* 2006; **66**: 1646-1658.
- Cheng J, Sun S, Tracy A, Hubbell E, Morris J, Valmeekam V et al. NetAffx Gene Ontology Mining Tool: a visual approach for microarray data analysis. *Bioinformatics* 2004; **20**: 1462-1463.
- Freeman WM, Walker SJ, Vrana KE. Quantitative RT-PCR: pitfalls and potential. *Biotechniques* 1999; **26**: 112-122, 24-5.
- Larionov A, Krause A, Miller W. A standard curve based method for relative real time PCR data processing. *BMC Bioinformatics* 2005; **6**: 62.
- Beloglazova N, Brown G, Zimmerman MD, Proudfoot M, Makarova KS, Kudritska M et al. A novel family of sequence-specific endoribonucleases associated with the clustered regularly interspaced short palindromic repeats. *J Biol Chem* 2008; **283**: 20361-20371.
- Nona CN, Guirguis S, Nobrega JN. Susceptibility to ethanol sensitization is differentially associated with changes in pCREB, trkB and BDNF mRNA expression in the mouse brain. *Behav Brain Res* 2013; **242**: 25-33.
- Lipina T, Labrie V, Weiner I, Roder J. Modulators of the glycine site on NMDA receptors, D-serine and ALX 5407, display similar beneficial effects to clozapine in mouse models of schizophrenia. *Psychopharmacology (Berl)* 2005; **179**: 54-67.
- Kim DH, Yoon BH, Kim YW, Lee S, Shin BY, Jung JW et al. The seed extract of *Cassia obtusifolia* ameliorates learning and memory impairments induced by scopolamine or transient cerebral hypoperfusion in mice. *J Pharmacol Sci* 2007; **105**: 82-93.



- 28 Wenk GL. Assessment of spatial memory using the radial arm maze and Morris water maze. *Curr Protoc Neurosci* 2004; **Chapter 8**: Unit 8.5A.
- 29 Yadav R, Gupta SC, Hillman BG, Bhatt JM, Stairs DJ, Dravid SM. Deletion of glutamate delta-1 receptor in mouse leads to aberrant emotional and social behaviors. *PLoS ONE* 2012; **7**: e32969.
- 30 Bottomly D, Walter NA, Hunter JE, Darakjian P, Kawane S, Buck KJ *et al*. Evaluating gene expression in C57BL/6 J and DBA/2 J mouse striatum using RNA-Seq and microarrays. *PLoS ONE* 2011; **6**: e17820.
- 31 Walter NA, McWeeney SK, Peters ST, Belknap JK, Hitzemann R, Buck KJ. SNPs matter: impact on detection of differential expression. *Nat Methods* 2007; **4**: 679–680.
- 32 Belforte JE, Zsiris V, Sklar ER, Jiang Z, Yu G, Li Y *et al*. Postnatal NMDA receptor ablation in corticolimbic interneurons confers schizophrenia-like phenotypes. *Nat Neurosci* 2010; **13**: 76–83.
- 33 Tseng KY, Chambers RA, Lipska BK. The neonatal ventral hippocampal lesion as a heuristic neurodevelopmental model of schizophrenia. *Behav Brain Res* 2009; **204**: 295–305.
- 34 Calejo AI, Reverendo M, Silva VS, Pereira PM, Santos MA, Zorec R *et al*. Differences in the expression pattern of HCN isoforms among mammalian tissues: sources and implications. *Mol Biol Rep* 2014; **41**: 297–307.
- 35 Spangler SA, Jaarsma D, De Graaff E, Wulf PS, Akhmanova A, Hoogenraad CC. Differential expression of liprin-alpha family proteins in the brain suggests functional diversification. *J Comp Neurol* 2011; **519**: 3040–3060.
- 36 Porta S, Marti E, de la Luna S, Arbones ML. Differential expression of members of the RCAN family of calcineurin regulators suggests selective functions for these proteins in the brain. *Eur J Neurosci* 2007; **26**: 1213–1226.
- 37 Scacheri PC, Rozenblatt-Rosen O, Caplen NJ, Wolfsberg TG, Umayam L, Lee JC *et al*. Short interfering RNAs can induce unexpected and divergent changes in the levels of untargeted proteins in mammalian cells. *Proc Natl Acad Sci USA* 2004; **101**: 1892–1897.
- 38 Fath S, Bauer AP, Liss M, Spriestersbach A, Maertens B, Hahn P *et al*. Multi-parameter RNA and codon optimization: a standardized tool to assess and enhance autologous mammalian gene expression. *PLoS ONE* 2011; **6**: e17596.
- 39 van den Buuse M. Modeling the positive symptoms of schizophrenia in genetically modified mice: pharmacology and methodology aspects. *Schizophr Bull* 2010; **36**: 246–270.
- 40 Wong AH, Josselyn SA. Caution when diagnosing your mouse with schizophrenia: the use and misuse of model animals for understanding psychiatric disorders. *Biol Psychiatry* 2016; **79**: 32–38.
- 41 Fabricius K, Helboe L, Fink-Jensen A, Wortwein G, Steiniger-Brach B. Pharmacological characterization of social isolation-induced hyperactivity. *Psychopharmacology (Berl)* 2011; **215**: 257–266.
- 42 Patil ST, Zhang L, Martenyi F, Lowe SL, Jackson KA, Andreev BV *et al*. Activation of mGlu2/3 receptors as a new approach to treat schizophrenia: a randomized Phase 2 clinical trial. *Nat Med* 2007; **13**: 1102–1107.



This work is licensed under a Creative Commons Attribution-NonCommercial-NoDerivs 4.0 International License. The images or other third party material in this article are included in the article's Creative Commons license, unless indicated otherwise in the credit line; if the material is not included under the Creative Commons license, users will need to obtain permission from the license holder to reproduce the material. To view a copy of this license, visit <http://creativecommons.org/licenses/by-nc-nd/4.0/>

© The Author(s) 2017

Supplementary Information accompanies the paper on the *Translational Psychiatry* website (<http://www.nature.com/tp>)